Robotica (2000) volume 18, pp. 33–41. Printed in the United Kingdom © 2000 Cambridge University Press

# A heuristic approach to grasp planning for a multifingered hand-arm robot based on the structure of empty space

Noriyuki Kawarazaki,* Tsutomu Hasegawa** and Kazue Nishihara*

**SUMMARY**

This paper proposes a grasp planning for a multifingered hand-arm robot in the presence of obstacles. When the hand grasps an object, neither the hand nor the arm should collide with obstacles. However, it is very difficult to generate a collision-free grasp configuration of the hand-arm robot due to its abundant degrees of freedom of motion. To overcome this difficulty, we first decompose the hand-arm robot into the multifingered hand part and the arm part. We develop two methods of the grasp planning. In one method, a collision-free configuration of the hand part is planned first. Then, the arm configuration is planned so as to enable the hand configuration. In the other method, the collision-free configuration of the arm part is planned first and the multifingered hand configuration second. The best method is selected according to the space structure of the environment. Various heuristics are developed to improve the efficiency of the planning and implementation of the system. Simulation results are presented.

KEYWORDS: Multifingered hand-arm robot; Grasp planning; Obstacle avoidance; Heuristics.

## 1. INTRODUCTION

This paper discusses a grasp planning for a multifingered hand-arm robot in the presence of obstacles. Since a multifingered hand-arm robot has many degrees of freedom of motion, it is a very time-consuming process to determine its grasp configuration even though geometric information about an object and obstacles is all known.

The grasp planning for a multifingered hand has been proposed in recent years. Guo, Gruver, and Jin[1] have derived the small displacement vibration equation for a multifingered robot hand based on the stiffness representation of grasping system. Omata and Farooqi[2] have developed a new method of regrasping by a multifingered hand to achieve a desired reorientation of an object by using regrasp primitives. Pollard and Lozano-Pérez[3] have proposed an algorithm to generate the grasp configuration for an arm with an articulated hand. Their plan was to find a set of fingertip contact points. They assumed that contact points would be on the faces of the object and that they knew which face each finger would contact. Pollard[4,5] has presented a partial solution to the problem of fitting a hand to an object in a given environment. The solution space for this problem is the 6-dimensional space of wrist configurations from which a specified type of collision-free grasp can be achieved. However, these plans only consider a multifingered hand robot, ignoring the arm part.

Our paper focuses on grasp planning for a whole multifingered hand-arm robot. Since determining the grasp configuration is a very time-consuming process, we use several heuristics in order to generate the grasp configuration rapidly. Two methods are developed for the grasp planning. In one method, a collision-free configuration of the hand part is planned first. Then, the arm configuration is planned so as to enable the hand configuration. In the other method, the collision-free configuration of the arm part is planned first and the multifingered hand configuration second. The most suitable method is selected according to the space structure of the environment. We divide the grasp planning into several subprocesses which are generating the grasp plane, determining the contact points, and generating the wrist position.[6–9]

This paper is organized as follows. The problem description of a grasp planning for a multifingered hand-arm robot is provided in Section 2. The procedure for generating the grasp configuration is described in Section 3. Section 4 proposes a grasp planning using several heuristics. Several implementation aspects are discussed in Section 5. Finally, conclusions are presented in Section 6.

## 2. PROBLEM DESCRIPTION

The problem addressed in this paper is to find a grasp configuration in which the hand can grasp an object and all intermediate links of the robot do not collide with obstacles. Before discussing the grasp planning, some basic assumptions need to be clarified.

- The kinematics of hand-arm robot and geometric information about an object and obstacles are all known.
- The multifingered hand-arm robot used here has a total of fifteen degrees of freedom of motion: six for the arm and nine for the hand (see Figure 1). The arm part is an articulated manipulator of the RPPRPR type. The hand part consists of a palm and three fingers, each with three joints. Each finger is the same RPP-type articulated manipulator and has a fingertip of hemisphere shape. The geometric relationship among the bases of the three fingers are the regular triangle shape.
- Three fingertips contact the surface of an object when the hand grasps the object with friction. Several conditions of stable grasp for the hand have to be satisfied. The finger can exert any force pointing within the friction cone at the point of contact. The effect of gravity is ignored to simplify the discussion.

* Dept. of System Design Engineering, Kanagawa Institute of Technology, Shimo-Ogino 1030, Atsugi, Kanagawa, (Japan)
** Graduate School of Information Science and Electrical Engineering, Kyushu University, 6-10-1 Hakozaki, Fukuoka, (Japan)

https://doi.org/10.1017/S0263574799002350 Published online by Cambridge University Press

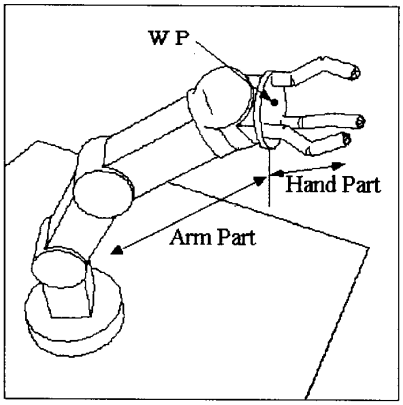



Fig. 1. Configuration of a Multifingered Hand-Arm.

- The object and all the obstacles are composed of polyhedra.

## 3. PROCEDURE FOR GENERATING THE GRASP CONFIGURATION

### *3.1. Grasp Plane (GP)*

When the hand grasps an object, three fingertips contact surfaces of the object. The plane defined based on the three contact points of the fingertips is called the grasp plane (GP) and is shown in Figure 2. Since the three contact points of the fingertips lie in the GP, the grasp configuration of the hand-arm robot depends on the GP. The GP is generated if the normal vector n and the grasp center point (GCP) are given. Since the hand must not collide with obstacles, we determine the GP in order for the hand to be located in the empty space. As shown in the next chapter, we determine the normal vector n and GCP based on the structure of empty space around the object.

### *3.2. Contact Point (CP)*

Next, we determine the contact point (CP) of the fingertip required for a stable grasp of an object. Since the CP lies in the section of the object, we assume that the hand grasps the object under the following conditions (see Figure 3).

*F*1: The CP is placed at the middle point of each edge of the object's section.

*F*2: All of fingertip forces intersect at the GCP.

From condition F1, the number of candidates of CPs is the number of edges of the object's section. We determine the set of three CPs satisfying the necessary and sufficient conditions for the stable grasp.

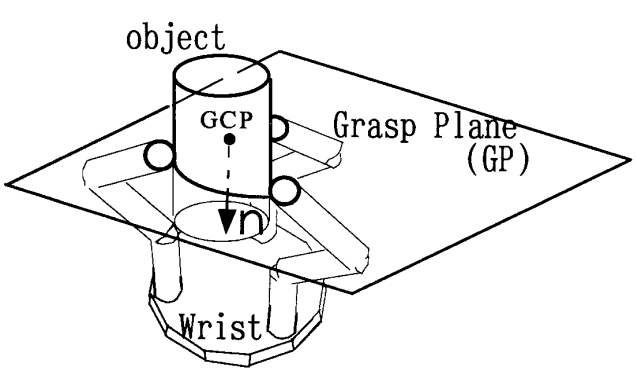



Fig. 2. Grasp plane (GP).

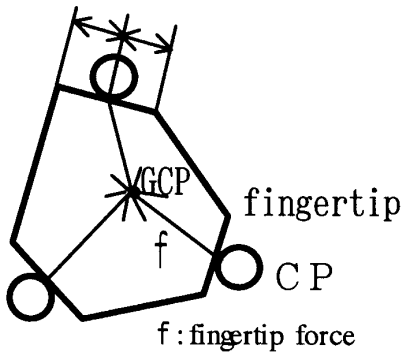



Fig. 3. Section of an object.

**Necessary and Sufficient Conditions for a Stable Grasp.** Previous researches on achieving a stable grasp for a multifingered hand have been reported.[10–13] We consider the static equilibrium of fingertip forces and the effect of the Coulomb friction. The effect of gravity is ignored to simplify the discussion. In order to consider the effect of gravity, we can expand the conditions for the stable grasp. The expanded conditions are discussed in Appendix A. The conditions for the stable grasp, as presented by Yoshikawa et al.,[14–15] are shown below.

*Condition C*1:
The total moment of the fingertip forces is zero.
*Condition C*2:
The total force of the fingertip forces is zero.
*Condition C*3:
Each fingertip force is in the friction cone.

Condition *C*1 is satisfied by the assumption F2. Since all fingertip forces point in the direction of the GCP, the moment is zero with respect to the GCP.

Condition *C*2 means the equilibrium of fingertip forces, which is shown below.

$$\begin{aligned} e_i^T(e_j + e_k) \le 0 \\ e_j^T(e_i + e_k) \le 0 \\ e_k^T(e_i + e_j) \le 0 \end{aligned} \tag{1}$$

where $e_i$: unit vector of fingertip force $f_i$

The unit vector of the fingertip force is determined based on assumptions *F*1 and *F*2.

The third condition, *C*3, is a restriction about Coulomb friction. Since we assume that each fingertip contacts the object with friction at a point, each fingertip force has to lie within the friction cone (see Figure 4). In the case of three-dimensional object, we calculate the friction cone as an area projected on the GP. From the assumption *F*2, the fingertip force vector points in the direction of the GCP. In order that the fingertip can contact an object without slippage, the fingertip force vector $f$ has to lie in the projected area shown as the oblique lines in Figure 4. This projected area depends on the friction coefficient and the angle between the GP and the object's surface.

https://doi.org/10.1017/S0263574799002350 Published online by Cambridge University Press

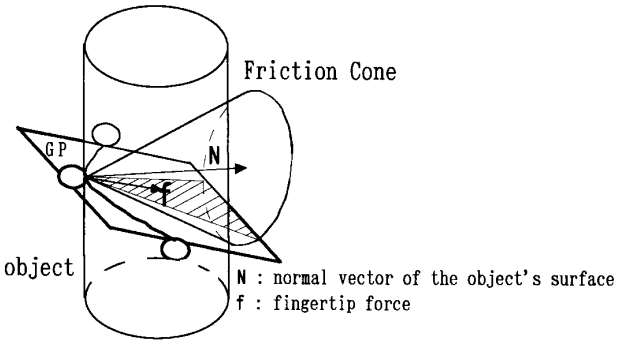



Fig. 4. Friction cone.

### *3.3. Wrist Position (WP)*

After generation of the GP and CP, we determine a feasible wrist position (WP). The location of the WP is planned at the grasp distance L from the GCP. We use 80% of the length of the finger as the value for L. There are two cases in which the multifingered hand grasps the object. In one case, the surface of the wrist intersects at the right angle with the normal vector n of the GP (see Figure 5(a)). The WP is placed in the direction of normal vector n. In the other case, the surface of the wrist does not intersect at the right angle with the normal vector n of the GP (see Figure 5(b)). The WP is placed in the direction of arbitrary vector n′. Many candidates of WPs are generated from one GP based on the arbitrary vector n′ and the grasp distance L.

As shown in Figure 6, the geometric relationship between vector n and vector n′ is described by two parameter angles $\alpha$ and $\beta$, the rotation angles about the Z and Y′ axis. Possible ranges of two parameter angles depend on the size of the hand. We generate several WPs and check whether or not the arm configuration based on the WP causes collision with obstacles.

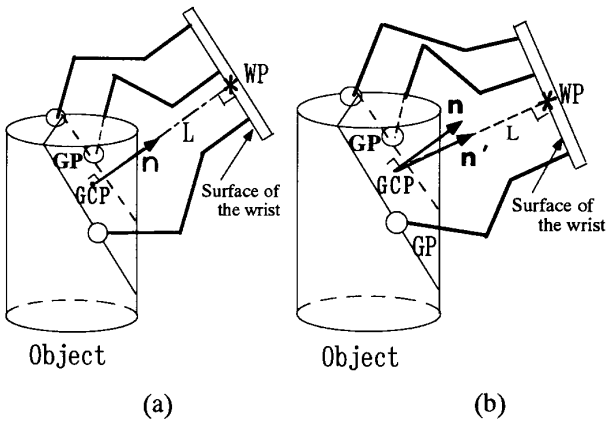



Fig. 5. Relationship between GP and WP.

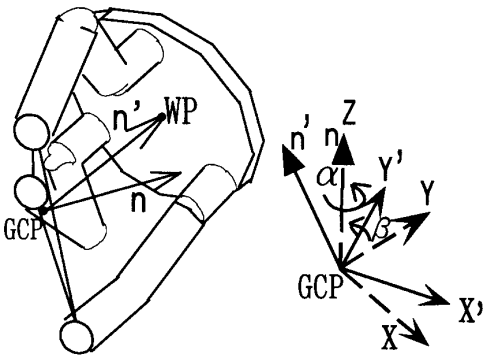



Fig. 6. Relationship between n and n′.

## 4. GRASP PLANNING USING HEURISTICS

**Heuristics Using the Situation of Placement of Obstacles.** It is very difficult to generate the collision-free grasp configuration of the multifingered hand-arm robot due to its abundant degrees of freedom of motion. To overcome this difficulty, we decompose the hand-arm robot into the multifingered hand part and the arm part. We developed two methods of the grasp planning. One method is called the hand-configuration method (HCM). The HCM plans a collision-free configuration of the hand part first, and then the arm configuration is planned so as to enable the hand configuration. In the other method, called the arm-configuration method (ACM), the collision-free configuration of the arm part is planned first and the multifingered hand configuration second. The best method is selected according to the space structure of the environment (see Figure 7).

**Heuristics Using the Structure of an Empty Space.** We assumed a complex environment in which many obstacles are put around an object. The hand-arm robot approaches the object from an empty space in order to avoid collisions with obstacles. In both methods, HCM and ACM, we use heuristics using the structure of the empty space around the object.

### *4.1. Ratio of the occupied space*

As shown in Figure 8(a), we define the WP space, which is a rectangular prism whose sides are located at finger's length $L_f$ away from vertices of the object space. The object space is the minimum rectangular prism including the object. The WP is located within the WP space so that fingertips reach at the surface of the object. We define the ratio of the occupied space in order to select either the HCM or the ACM. If the ratio of the occupied space exceeds the threshold, we use the HCM to generate the grasp configuration. If the ratio of the occupied space does not exceed the

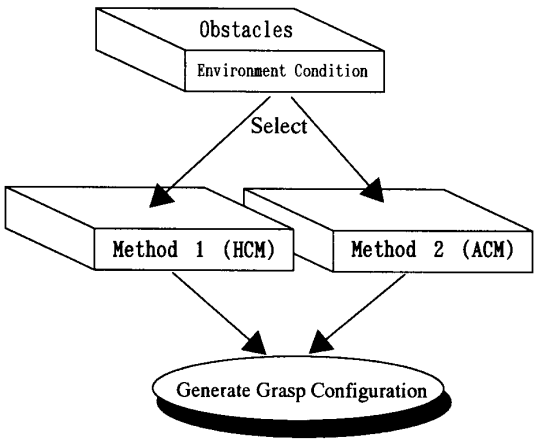
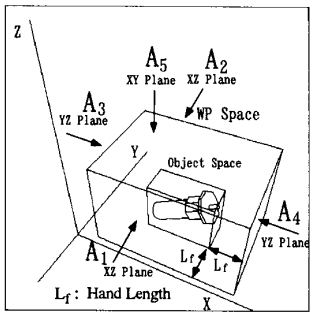


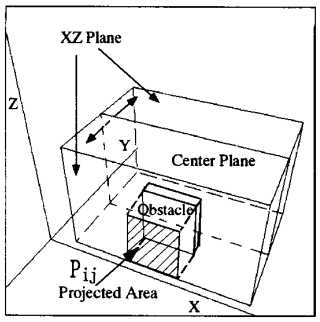

Fig. 7. General flow of the grasp planning.

https://doi.org/10.1017/S0263574799002350 Published online by Cambridge University Press




(a)

Fig. 8. (a) WP space.




(b)

Fig. 8. (b) Projected area.

threshold, we use the ACM. In order to evaluate the occupied space, we use the obstacle's projected area on the surface of the WP space. The ratio of the occupied space is shown below.

$$C = \frac{\sum_{i=1}^{5} \sum_{j=1}^{n} S(P_{ij})}{\sum_{i=1}^{5} S(A_i)} \qquad (2)$$

where

$P_{ij} = P(A_i, B_j)$

$A_i$ : i-th boundary in the WP space
$B_j$ : j-th obstacle
$P_{ij}$ : $B_j$'s area which is projected on the $A_i$ plane
S : area
n : number of obstacles

The actual procedure to calculate the obstacle's projected area is shown in Figure 8(b). The obstacle which is placed between the center plane and the XZ plane is projected on the XZ plane. The same procedure is followed to calculate the projected area on other planes of WP space.

### *4.2. Hand-configuration method*

The Hand-configuration method (HCM) gives priority to generate the hand configuration. The algorithm of the HCM is as follows:

Step 1: Candidates of the grasp center point (GCP) are generated in the object. End as failure if new candidates of GCP are not generated.

Step 2: The priority about each candidate of GCP is determined based on the structure of the empty space around the object.
The Grasp Plane (GP) is determined based on the selected GCP and the structure of the empty space around the object.

Step 3: We attempt to generate the hand configuration according to the selected GP. After generation of the hand configuration, we attempt to generate the arm configuration. End successfully if the grasp configuration is generated, else go to Step 1.

**Procedure for generating of candidates of GCP.** Candidates of GCP are generated by the following recursive procedure.

(i) The object space, which is the minimum rectangular prism including the object, is generated.
(ii) As shown in Figure 9, the object space is divided equally into eight smaller rectangular prisms. Those vertices of the rectangular prism, which are included in the object, are chosen as candidates of the GCP.
(iii) If the grasp configuration is not generated based on the obtained candidates of GCP, each rectangular prism is subdivided equally into eight and new candidates of GCP are generated.
The procedure ends as failure if the shortest edge of the subdivided rectangular prism is shorter than the threshold.

**GP based on the structure of empty space.** To evaluate the structure of the empty space around the object, we use a geodesic dome and a distance transformation.[16] The geodesic dome consists of facets with an almost identical triangular shape. The initial geodesic dome is an icosahedron with 20 facets. The geodesic domes are constructed by recursively subdividing a triangular facet into four smaller facets. Thus, the local space is divided uniformly into triangular pyramids, each with a vertex located at the center of the dome and with one of the triangular facets of the geodesic dome as its base (see Figure 10).

The geodesic dome whose center point is the candidate of the GCP is generated. The priority about each candidate of GCP is determined by the number of good triangular

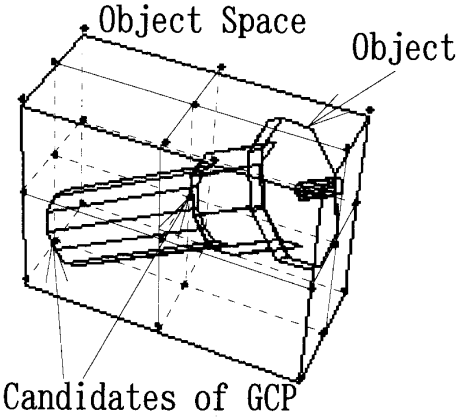



Fig. 9. Candidates of GCP.

https://doi.org/10.1017/S0263574799002350 Published online by Cambridge University Press

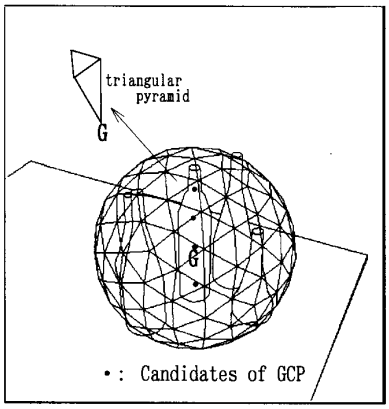



Fig. 10. Geodesic dome.

pyramids of the geodesic dome. A good triangular pyramid must satisfy the following conditions.

(i) The triangular pyramid does not collide with obstacles.
(ii) The center point of the base of the triangular pyramid does not collide with an object.
(iii) The center point of the base of the triangular pyramid is within the motion range of the tip of the robot arm.

We use the center point of the base of the triangular pyramid as the WP. Therefore condition (iii) means the feasibility of the WP.

Triangular pyramids are classified into two kinds: colliding and non-colliding ones. To identify the direction of the most widely open space, the distance transformation is applied to the non-colliding pyramids with respect to the colliding pyramids. The distance between triangular facets on the surface of the geodesic dome is defined as the distance between the triangular pyramids. As shown in Figure 11, those facets with oblique lines are colliding pyramids, and the number on the other facets indicates the distance value. The triangular pyramid with the largest value is the center of the most widely open space. The normal vector of the triangular facet of this pyramid is chosen as the most appropriate normal vector $n$ of the GP (see Figure 12).

### *4.3. Arm-configuration method (ACM)*

The arm-configuration method (ACM) gives priority to generate the arm configuration. The algorithm of the ACM is as follows.

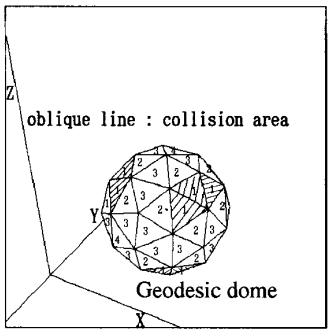



Fig. 11. Distance transformation.

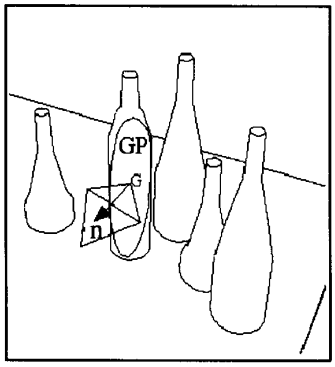



Fig. 12. GP and triangular pyramid.

Step 1: Candidates of the wrist position (WP) are generated in the WP space. End as failure if new candidates of WP are not generated.
Step 2: The priority about each candidate of WP is determined based on the number of good triangular pyramids of the geodesic dome.
Step 3: We attempt to generate the arm configuration according to the selected WP. After generation of the arm configuration, we attempt to generate the hand configuration. End successfully if the grasp configuration is generated, else go to Step 1.

**Procedure for generating of candidates of WP.** Candidates of WP are generated by the following recursive procedure.

(i) The WP space, which is defined in Chapter 4.1, is generated.
(ii) As shown in Figure 13, the WP space is divided equally into eight smaller rectangular prisms. Those vertices of the rectangular prism, which are not included in the object and obstacles, are chosen as candidates of the WP.
(iii) If the grasp configuration is not generated based on the obtained candidates of WP, each rectangular prism is subdivided equally into eight and new candidates of WP are generated.
The procedure ends as failure if the shortest edge of the subdivided rectangular prism is shorter than the threshold.

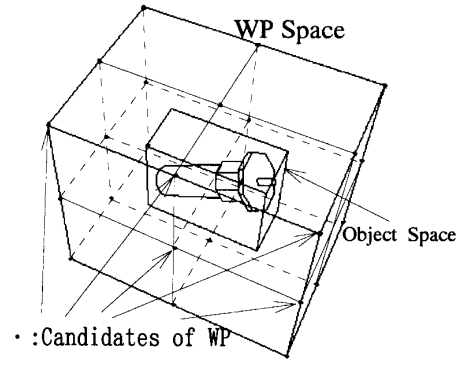



Fig. 13. Candidates of WP.

https://doi.org/10.1017/S0263574799002350 Published online by Cambridge University Press

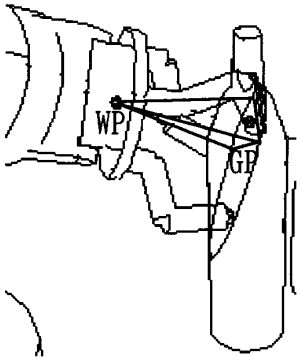



Fig. 14. WP and triangular pyramid.

**WP based on the geodesic dome.** The geodesic dome whose center point is the candidate of the WP is generated. The priority about each candidate of WP is determined by the number of good triangular pyramids of the geodesic dome. A good triangular pyramid must satisfy the following conditions:

(i) The base of the triangular pyramid is included in the object.
(ii) The arm configuration determined by the triangular pyramid does not collide with any obstacles.

Since the top of the arm faces the direction from the WP to the GCP, the arm configuration can be obtained geometrically on the basis of the WP and the triangular pyramid. The geometric relationship between the WP and the GP is generated based on the triangular pyramid of the geodesic dome (see Figure 14). The WP is the top of the triangular pyramid, and the GP is the center point of the base of the triangular pyramid.

## 5. SIMULATION RESULTS

We made simulations in order to clarify the effectiveness of our proposed algorithm (see Figure 15). The object to be grasped is an electric motor. In example 1, several boards are placed as obstacles around the object. In example 2, an arch and a rectangular prism are placed as obstacles around the object. The ratio of the occupied space is calculated for each example in order to determine the best method for generating the grasp configuration. Since the ratio of the occupied space of example 1 exceeds the threshold and that of example 2 is smaller than the threshold, the HCM and the ACM are used respectively (see Figure 15). We set the threshold at 0.2.

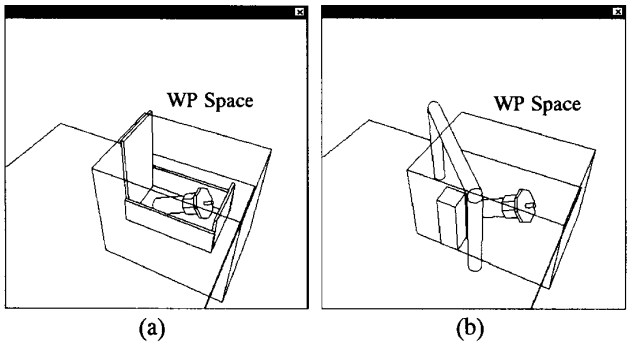



Fig. 15. Simulation results.
(a) Example 1 (C = 0.26). (b) Example 2 (C = 0.07).

*Example 1*

Each step of HCM is shown in Figure 16(a)–(f). At the first step, several candidates of the GCP are obtained within the object (see Figure 16(a)). The geodesic dome is generated around each candidate of the GCP in order to analyze the structure of the empty space (see Figure 16(b)). We determine the priority of GCP based on the structure of the empty space around each candidate of the GCP. Many GPs are generated based on the empty space analysis using the triangular pyramids of the geodesic dome . The total number of candidates of GPs is 320. From those GPs, a good GP is selected based on the distance transformation (see Figure 16(c)). The section of the object is shown in Figure 16(d). The triangle shape in Figure 16(d) shows connected lines among three CPs. The obtained grasp configuration is shown in Figure 16(e). The multifingered hand-arm robot avoids collision and can grasp the object. A detailed situation of grasping the object is shown in Figure 16(f). It is shown that the hand grasps the object stably.

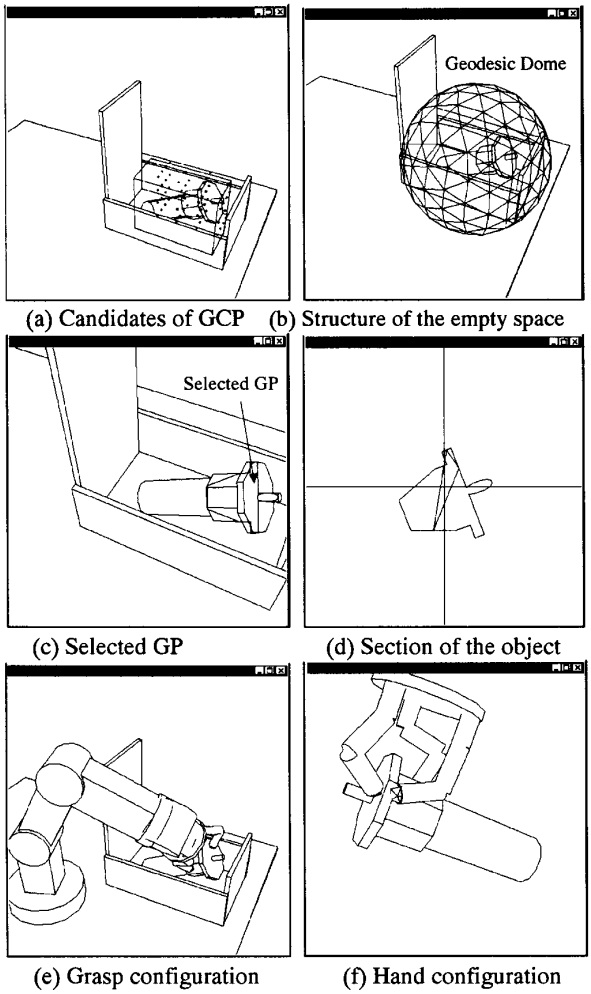



Fig. 16. Simulation results (HCM)
(a) Candidates of GCP. (b) Structure of the empty space. (c) Selected GP. (d) Section of the object. (e) Grasp configuration. (f) Hand configuration.

https://doi.org/10.1017/S0263574799002350 Published online by Cambridge University Press

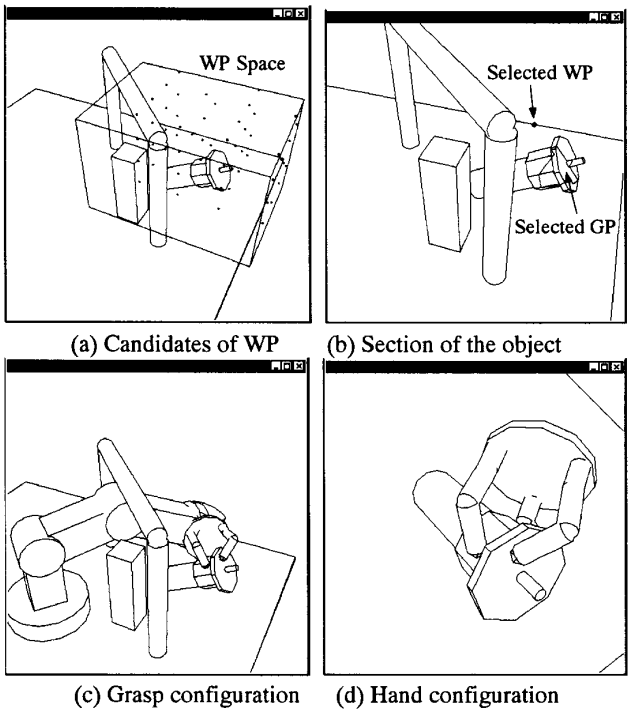



Fig. 17. Simulation results (ACM).
(a) Candidates of WP. (b) Section of the object. (c) Grasp configuration. (d) Hand configuration.

*Example 2*
Each step of ACM is shown in Figure 17(a)–(d). At the first step, several candidates of the WP are obtained within the WP space (see Figure 17(a)). The geodesic dome is generated around each candidate of the WP in order to analyze the structure of the empty space. We determine the priority of WP according to the number of good triangular pyramids of the geodesic dome. Many GPs are generated based on the triangular pyramid of the geodesic dome. Among those GPs, a good GP is selected based on the structure of the empty space around the object. The selected WP and GP are shown in Figure 17(b). The obtained grasp configuration is shown in Figure 17(c). A detailed situation of grasping the object is shown in Figure 17(d). It is shown that the hand grasps the object stably.

**The Effectiveness of Heuristics.** In order to evaluate the effectiveness of heuristics, we compare computing times for generating the grasp configuration in different situations. Table I shows the computing times of example 1 and example 2. These are obtained based on HCM and ACM respectively. In Table I, underline presents the selected method based on the ratio of the occupied space. In both examples, the grasp configuration is generated rapidly by the selected method. Table II shows the computing times for example 1. There are four different cases. The computing time of Case 4 is ten times as much as that of Case 1.

Table I. Comparison of computing time 1

| | ACM | HCM |
|---|---|---|
| Example 1 | 5′ 43″ | 4′ 32″ |
| Example 2 | 7′ 35″ | 14′ 22″ |

(underline: selected method)

Table II. Comparison of computing time 2

| | Case 1 | Case 2 | Case 3 | Case 4 |
|---|---|---|---|---|
| Example 1 | 4′ 32″ | 14′ 7″ | 10′ 17″ | 39′ 49″ |

Case 1: HCM
Case 2: HCM without priority of GCP based on the geodesic dome
Case 3: HCM without priority of GCP based on the distance transformation
Case 4: HCM without priority of GCP based on the geodesic dome and distance transformation

Table III shows the computing times for example 2. The computing time of ACM without WP priority is two times as much as that of ACM.

## 6. CONCLUSIONS

In this paper, we proposed a grasp planning for a multifingered hand-arm robot in the presence of obstacles. We use several heuristics in order to generate the grasp configuration rapidly. We propose two methods which are called the hand-configuration method (HCM) and the arm-configuration method (ACM). We select one method according to the ratio of the occupied space defined on the basis of the space structure of the environment. In both methods, we use the heuristics of the structure of the empty space around the object. In order to evaluate the structure of the empty space around the object, we use the geodesic dome and the distance transformation. We divide the grasp planning into several subprocesses, generating the grasp plane (GP), determining the contact point (CP), and generating the wrist position (WP). The actual grasp configuration is generated based on the obtained CP and WP. The effectiveness of our method and the advantage of heuristics are clarified by computer simulations.

## APPENDIX A: EXPANDED CONDITIONS OF STABLE GRASP

In order to take the effect of gravity into consideration, necessary and sufficient conditions of stable grasp are expanded[14,15] as follows:

**Condition C′1:.** The total moment of the fingertip forces and gravity is zero.

Table III. Comparison of computing time 3

| | ACM | without WP priority |
|---|---|---|
| Example 2 | 7′ 35″ | 14′ 32″ |

https://doi.org/10.1017/S0263574799002350 Published online by Cambridge University Press

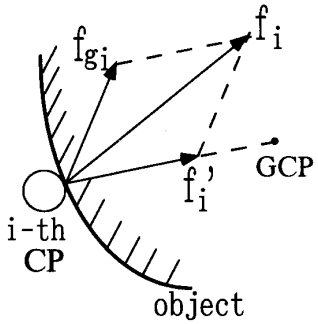



Fig. A1. Fingertip force.

**Condition C′2:.** The total force of the fingertip forces and gravity is zero.

**Condition C′3:.** Each fingertip force is in the friction cone.

As shown in Figure A1, we define that the fingertip force $f_i$ consists of $f_{gi}$ and $f_i'$. The total force of three $f_{gi}$ balances with gravity. Each of the three $f_i'$ point in the direction of the GCP.

The fingertip force $f_i$ is shown below.

$$f_i = f_{gi} + f_i' \quad (i = 1, 2, 3) \tag{A1}$$

Fingertip force $f_{gi}$ satisfies following the equations.

$$\begin{cases} -mg = \sum_{i=1}^{3} f_{gi} \text{ (balance of force)} \\ -rg \times mg = \sum_{i=1}^{3} (r_i \times f_{gi}) \text{ (balance of moment)} \end{cases} \tag{A2}$$

m: mass of object
g: acceleration of gravity
$r_i = [r_{ix}\ r_{iy}\ r_{iz}]^T$: position vector of i-th CP

Fingertip force Fg, which is balanced with the gravity, is obtained on the basis of the following equations.

$$F_g = [f_{g1}^T\ f_{g2}^T\ f_{g3}^T] = -A^+ T \tag{A3}$$

where

$$A = \begin{Bmatrix} 1 & 0 & 0 & 1 & 0 & 0 & 1 & 0 & 0 \\ 0 & 1 & 0 & 0 & 1 & 0 & 0 & 1 & 0 \\ 0 & 0 & 1 & 0 & 0 & 1 & 0 & 0 & 1 \\ 0 & -r_{1z} & r_{1y} & 0 & -r_{2z} & r_{2y} & 0 & -r_{3z} & r_{3y} \\ r_{1z} & 0 & -r_{1x} & r_{2z} & 0 & -r_{2x} & r_{3z} & 0 & -r_{3x} \\ -r_{1y} & r_{1x} & 0 & -r_{2y} & r_{2x} & 0 & -r_{3y} & r_{3x} & 0 \end{Bmatrix}$$

+: pseudoinverse matrix

$$T = \begin{Bmatrix} 0 \\ 0 \\ mg \\ mg \times r_{gy} \\ -mg \times r_{gx} \\ 0 \end{Bmatrix}$$

$r_g = [r_{gx}\ r_{gy}\ r_{gz}]^T$: position vector of object's center of gravity

Since the total fingertip forces $f_{gi}$ is balanced with the gravity, we consider the remaining element $f_i'$ of fingerfip force $f_i$. Then, conditions C′1 and C′2 are the same as conditions C1 and C2.

Since all fingertip forces $f_i'$ point in the direction of the GCP, the moment is zero with respect to the GCP, and condition C'1 is satisfied.

Condition C′2 is shown below.

$$\begin{aligned} e_i'^T (e_j' + e_k') \le 0 \\ e_j'^T (e_i' + e_k') \le 0 \\ e_k'^T (e_i' + e_j') \le 0 \end{aligned} \tag{A4}$$

where $e_i'$: unit vector of fingertip force $f_i'$

Condition C′3 is concerned with fingertip force f. The equation of condition C′3 is shown below.

$$e_i^T n_i > \frac{1}{\sqrt{1 + \tan^2 \alpha_i}} \tag{A5}$$

where $e_i$: unit vector of fingertip force $f_i$
$n_i$: normal vector of object's surface
$\alpha_i$: angle of friction at i-th CP

## References


1. Gongliang Guo, William A. Gruver and Kai Jin, "Grasp Planning for Multifingered Robot Hands," *Proc. IEEE Int. Conf. on Robotics and Automation* (1992) pp. 2284–2289.
2. Toru Omata and Mohammad Asim Farooqi, "Regrasps by a Multifingered Hand based on Primitives", *Proc. IEEE Int. Conf. on Robotics and Automation* (1996) pp. 2774–2780.
3. Nancy S. Pollard and T. Lozano-Pérez, "Grasp Stability and Feasibility for an Arm with an Articulated Hand", *Proc. IEEE Int. Conf. on Robotics and Automation* (1990) pp. 1581–1585.
4. Nancy S. Pollard, "Planning Grasps for a Robot Hand in the Presence of Obstacles," *Proc. IEEE Int. Conf. on Robotics and Automation* (1993) pp. 723–728.
5. Nancy S. Pollard, "Parallel Algorithms for Synthesis of Whole-Hand Grasps", *Proc. IEEE Int. Conf. on Robotics and Automation* (1997) pp. 373–378.
6. Noriyuki Kawarazaki, Tsutomu Hasegawa and Kazue Nishihara, "Grasp Planing for a Multifingered Hand-Arm Robot in the Presence of Obstacles", *Proc. of the 2nd Int. Workshop on Advanced Mechatronics* (1997) pp. 214–219.
7. Noriyuki Kawarazaki, Tsutomu Hasegawa and Kazue Nishihara, "Grasp Planning Algorithm for a Multifingered Hand-Arm Robot, *Proc. IEEE Int. Conf. on Robotics and Automation* (1998) pp. 933–939.
8. Noriyuki Kawarazaki, Tsutomu Hasegawa and Kazue Nishihara, "Grasp Planning for a Multifingered Hand-Arm Robot in Consideration of the Structure of Empty Space, *Proc. of the 5th Int. Conf. on Intelligent Autonomous Systems* (1998) pp. 496–503.
9. Noriyuki Kawarazaki, Tsutomu Hasegawa and Kazue Nishihara, "A Heuristic Method for Finding the Grasp Configuration of Multifingered Hand-Arm Robot", *Proc. of the 14th Int. Conf. on Computer-Aided Production Engineering* (1998) pp. 475–480.
10. Jeffrey Kerr and Bernard Roth, " Analysis of Multifingered Hands", *Int. J.Robotics Research*, **4**, No. 4, 3–17 (1986).
11. Van-Duc Nguyen, "Constructing Stable Grasps in 3D", *Proc. IEEE Int. Conf. on Robotics and Automation* (1987) pp. 234–239.
12. Van-Duc Nguyen, "Constructing Stable Grasps", *Int. J. Robotics Research*, **8**, No.1, 26–37 (1989).


https://doi.org/10.1017/S0263574799002350 Published online by Cambridge University Press

13. Jean Ponce and Bernard Faverjon, “On Computing Three-Finger Force-Closure Grasps of Polygonal Objects” *IEEE Trans. on Robotics and Automation*, **11** No.6, 868–881, (Dec.1995).
14. Tsuneo Yoshikawa, Yasuyoshi Yokokohji and Atsuo Nagayama, “Object Handling by Three-Fingered Hands Using Slip Motion”, *Journal of the Robotics Society of Japan*, **10** No. 3, 394–401 (1992) (in Japanese).
15. Tsuneo Yoshikawa and Kiyoshi Nagai, “Manipulating and Grasping Forces in Manipulation by Multifingered Robot Hands”, *IEEE Int. Trans. on Robotics and Automation*, **7** No.1, 67–77 (Feb. 1991).
16. H.Onda, T.Hasegawa and T. Matsui, “Collision Avoidance for a 6-DOF Manipulator Based on Empty Space Analysis of the 3-D Real World,” *Proc. IEEE Int. Workshop on Intelligent Robots and Systems IROS* ’91 (1991) pp. 583–589.

https://doi.org/10.1017/S0263574799002350 Published online by Cambridge University Press